Available online at www.sciencedirect.com
SCIENCE DIRECT®

Global and Planetary Change 39 (2003) 201–213

GLOBAL AND PLANETARY CHANGE

www.elsevier.com/locate/gloplacha

Continental-scale comparisons of terrestrial carbon sinks estimated from satellite data and ecosystem modeling 1982–1998

Christopher Potter[a,*], Steven Klooster[b], Ranga Myneni[c], Vanessa Genovese[b], Pang-Ning Tan[d], Vipin Kumar[d]

[a] NASA Ames Research Center, Moffett Field, CA 94035, USA
[b] California State University Monterey Bay, Seaside, CA, USA
[c] Boston University, Boston, MA, USA
[d] University of Minnesota, Minneapolis, MN, USA

Received 25 June 2002; received in revised form 14 January 2003; accepted 29 January 2003

Abstract

A simulation model based on satellite observations of monthly vegetation cover was used to estimate monthly carbon fluxes in terrestrial ecosystems from 1982 to 1998. The NASA–CASA model was driven by vegetation properties derived from the Advanced Very High Resolution Radiometer (AVHRR) and radiative transfer algorithms that were developed for Moderate Resolution Imaging Spectroradiometer (MODIS). For the terrestrial biosphere, predicted net ecosystem production (NEP) flux for atmospheric CO_2 has varied widely between an annual source of −0.9 Pg C per year and a sink of +2.1 Pg C per year. The southern hemisphere tropical zones (SHT, between 0° and 30°S) have a major influence over the predicted global trends in interannual variability of NEP. In contrast, the terrestrial NEP sink for atmospheric CO_2 on the North American (NA) continent has been fairly consistent between +0.2 and +0.3 Pg C per year, except during relatively cool annual periods when continental NEP fluxes are predicted to total to nearly zero. The predicted NEP sink for atmospheric CO_2 over Eurasia (EA) increased notably in the late 1980s and has been fairly consistent between +0.3 and +0.55 Pg C per year since 1988. High correlations can be detected between the El Niño Southern Oscillation (ENSO) and predicted NEP fluxes on the EA continent and for the SHT latitude zones, whereas NEP fluxes for the North American continent as a whole do not correlate strongly with ENSO events over the same time series since 1982. These observations support the hypothesis that regional climate warming has had notable but relatively small-scale impacts on high latitude ecosystem (tundra and boreal) sinks for atmospheric CO_2.
Published by Elsevier B.V.

Keywords: Carbon dioxide; Ecosystems; Remote sensing; Ocean climate

1. Introduction

Less than 50% of the carbon emitted to the atmosphere each year through forest loss, fossil fuel combustion, and industrial activities remains in the atmosphere. The remainder of the carbon emitted through these human activities is reabsorbed and stored as sinks, perhaps temporarily, in the oceans and in terrestrial ecosystems (Schimel et al., 2001). This is the so-called "missing sink" for carbon dioxide emissions. Measured atmospheric CO_2, ^{13}C, and O_2/N_2 distributions indicate that during the past 2

* Corresponding author. Tel.: +1-650-604-6164; fax: +1-650-604-4680.
E-mail address: cpotter@gaia.arc.nasa.gov (C. Potter).

0921-8181/$ - see front matter. Published by Elsevier B.V.
doi:10.1016/j.gloplacha.2003.07.001

decades, a large fraction of the missing carbon sink has been on land (Bender et al., 1996; Keeling et al., 1996; Rayner et al., 1999), specifically in the temperate and boreal latitudes of the Northern Hemisphere. Nevertheless, the mechanisms and the precise spatial pattern of a sink for CO_2 in the terrestrial biosphere remain uncertain, to a large degree because the heterogeneity of land cover and ecosystem exchange processes have not been measured in adequate detail to determine precise regional sink contributions for atmospheric CO_2 (USGCRP, 1999; Watson et al., 2000).

Uncertainties in terrestrial carbon fluxes may be reduced with the development of improved modeling techniques for estimating variability in ecosystem processes over vast land areas (IGBP, 1998). Global ecosystem models (e.g., Maisongrande et al., 1995; Kindermann et al., 1996; McGuire et al., 2001) are valuable tools in situations when ground-based measurements of carbon fluxes are not adequate to realistically capture variability on a regional basis. A computer model of this type based on satellite measurements of vegetation cover has been developed to simulate global ecosystem carbon cycling (Potter and Klooster, 1997, 1998; Potter, 1999). Our NASA–Carnegie Ames Stanford Approach (CASA) model is designed to estimate monthly patterns in carbon fixation, plant biomass, nutrient allocation, litter fall, soil nutrient mineralization, and CO_2 exchange, including carbon emissions from soils worldwide.

Direct input of satellite "greenness" data from the Advanced Very High Resolution Radiometer (AVHRR) sensor into the NASA–CASA model is used to estimate spatial variability in monthly net primary production (NPP), biomass accumulation, and litter fall inputs to soil carbon pools at a geographic resolution of 0.5° latitude/longitude. Global NPP of vegetation is predicted using the relationship between greenness reflectance properties and the fraction of absorption of photosynthetically active radiation (FPAR), assuming that net conversion efficiencies of PAR to plant carbon can be approximated for different ecosystems or are nearly constant across all ecosystems (Sellers et al., 1994; Running and Nemani, 1998; Goetz and Prince, 1998). In this study, we compare the results of NASA–CASA model predictions from 1982 to 1998 to infer variability in continental-scale carbon fluxes and to understand global climate control patterns over terrestrial carbon sinks.

2. Modeling methods and global drivers

As documented in Potter (1999), the monthly NPP flux, defined as net fixation of CO_2 by vegetation, is computed in NASA–CASA on the basis of light-use efficiency (Monteith, 1972). Monthly production of plant biomass is estimated as a product of time-varying surface solar irradiance S_r and FPAR from the satellite AVHRR, plus a constant light utilization efficiency term (e_{max}) that is modified by time-varying stress scalar terms for temperature (T) and moisture (W) effects (Eq. (1)):

$$\mathrm{NPP} = S_r \mathrm{FPAR}\ e_{max} T\ W \tag{1}$$

The e_{max} term is set uniformly at 0.39 g C MJ^{-1} PAR, a value that derives from calibration of predicted annual NPP to previous field estimates (Potter et al., 1993). This model calibration has been validated globally by comparing predicted annual NPP to more than 1900 field measurements of NPP (Fig. 1). Interannual NPP fluxes from the CASA model have been reported (Behrenfeld et al., 2001) and validated against multi-year estimates of NPP from field stations and tree rings (Malmström et al., 1997).

The T stress scalar is computed with reference to derivation of optimal temperatures (T_{opt}) for plant production. The T_{opt} setting will vary by latitude and longitude, ranging from near 0 °C in the Arctic to the middle 30 in low-latitude deserts. The W stress scalar is estimated from monthly water deficits, based on a comparison of moisture supply (precipitation and stored soil water) to potential evapotranspiration (PET) demand using the method of Priestly and Taylor (1972).

Evapotranspiration is connected to water content in the soil profile layers (Fig. 2), as estimated using the NASA–CASA algorithms described by Potter (1999). The soil model design includes three-layer (M_1–M_3) heat and moisture content computations: surface organic matter, topsoil (0.3 m), and subsoil to rooting depth (1–2 m). These layers can differ in soil texture, moisture holding capacity, and carbon–nitrogen dynamics. Water balance in the soil is modeled as the difference between precipitation or volumetric perco-

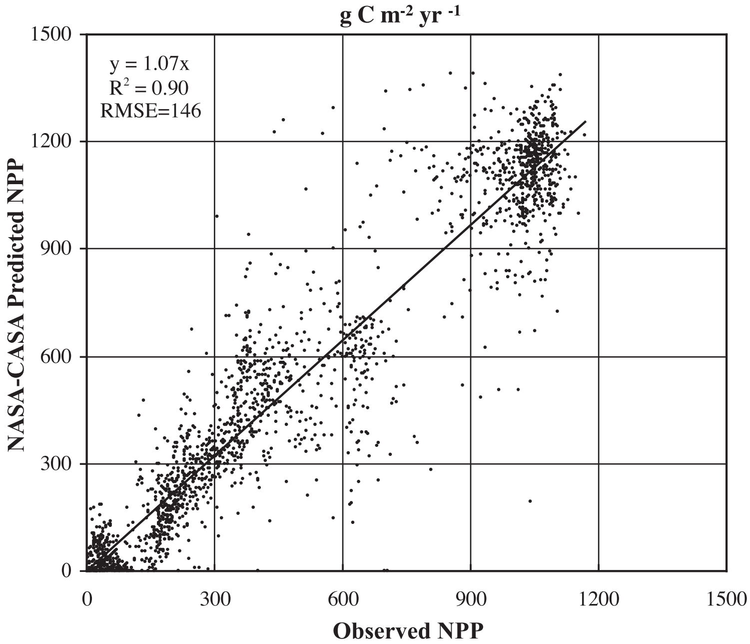

Fig. 1. Comparison of annual observed NPP to predicted values from the NASA–CASA model (driven by 0.5° FPAR from the satellite AVHRR and climate means from New et al., 2000). The data set of more than 1900 observed NPP points was compiled for the Ecosystem Model Data Intercomparison (EMDI) activity by the Global Primary Productivity Data Initiative (GPPDI) working groups of the International Geosphere Biosphere Program Data and Information System (IGBP-DIS; Olson et al., 1997).

lation inputs, monthly estimates of PET, and the drainage output for each layer. Inputs from rainfall can recharge the soil layers to field capacity. Excess water percolates to lower layers and may eventually leave the system as seepage and runoff. Freeze–thaw dynamics with soil depth operate according to the empirical degree–day accumulation method (Jumikis, 1966), as described by Bonan (1989).

Based on plant production as the primary carbon and nitrogen cycling source, the NASA–CASA model is designed to couple daily and seasonal patterns in soil nutrient mineralization and soil heterotropic respiration (R_h) of CO_2 from soils worldwide. Net ecosystem production (NEP) can be computed as NPP minus R_h fluxes, excluding the effects of small-scale fires and other localized disturbances or vegetation regrowth patterns on carbon fluxes (Walker and Steffen, 1997). The NASA–CASA soil model uses a set of compartmental difference equations with a structure comparable to the CENTURY ecosystem model (Parton et al., 1992). First-order decay equations simulate exchanges of decomposing plant residue (metabolic and structural fractions) at the soil surface. The model also simulates surface soil organic matter (SOM) fractions that presumably vary in age and chemical composition. Turnover of active (microbial biomass and labile substrates), slow (chemically protected), and passive (physically protected) fractions of the SOM are represented. Along with moisture availability and litter quality, the predicted soil temperature in the M_1 layer controls SOM decomposition. Soil fertility factors are included in the NASA–CASA model, which control the allocation of new plant growth to above ground tissues (leaf and wood) vs. fine root tissue allocation for acquisition of soil nutrients (Potter, 1999).

Whereas previous versions of the NASA–CASA model (Potter et al., 1993, 1999) used a normalized difference vegetation index (NDVI) to estimate FPAR, the current model version instead relies upon canopy radiative transfer algorithms (Knyazikhin et al., 1998), which are designed to generate improved FPAR products as inputs to carbon flux calculations. These radiative transfer algorithms, developed for the Moderate Resolution Imaging Spectroradiometer (MODIS) in-

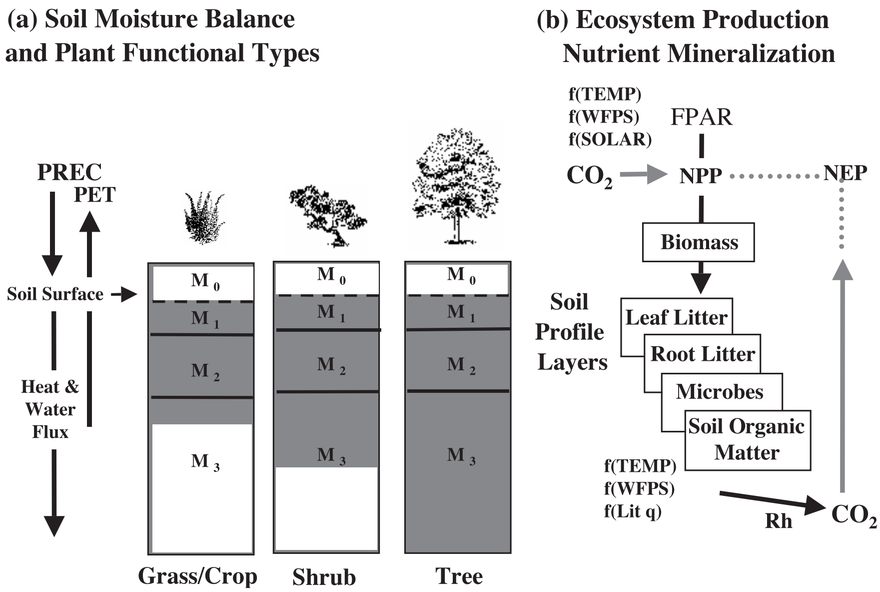

Fig. 2. Schematic representation of components in the NASA–CASA model. The soil profile component (a) is layered with depth into a surface ponded layer (M_0), a surface organic layer (M_1), a surface organic-mineral layer (M_2), and a subsurface mineral layer (M_3), showing typical levels of soil water content (shaded) in three general vegetation types. The production and decomposition component (b) shows separate pools for carbon cycling among pools of leaf litter, root litter, woody detritus, microbes, and soil organic matter. Microbial respiration rate is controlled by temperature (TEMP) and litter quality (q).

strument aboard the NASA Terra platform, account for attenuation of direct and diffuse incident radiation by solving a three-dimensional formulation of the radiative transfer process in vegetation canopies. Monthly composite data from channels 1 and 2 of the AVHRR have been processed according to the MODIS radiative transfer algorithms and aggregated over the global land surface to 0.5° resolution, consistent with the NASA–CASA climate driver data. To minimize cloud contamination effects, a maximum value composite algorithm was applied spatially for 0.5° pixel values.

Gridded climate drivers of mean monthly solar radiation, air surface temperature (TEMP), and precipitation (PREC) come from interpolated weather station records (New et al., 2000) distributed across all the continental masses. Land cover categories for vegetation types are derived from AVHRR classification products (DeFries et al., 1995).

The NASA–CASA soil carbon pools were initialized to represent storage and flux conditions in near steady state (annual NEP less than 0.5% of global annual NPP) with respect to mean land surface climate recorded for the period 1979–1981 (New et al., 2000). This initialization protocol was found to be necessary to eliminate any notable discontinuities in predicted NEP fluxes during the transition to our model simulation years of interest, which were run on a monthly time step starting January 1982 to December 1998 using interannual FPAR and climate drivers. When this soil carbon initialization step is not properly included, we note that an ecosystem model will likely predict artificially large carbon sinks in the terrestrial biosphere that then diminish as an artifact feature over the actual simulation period of interest as the model eventually approaches steady state. Initializing to near steady state does not, however, address the issue that some ecosystems are not in equilibrium with respect to net annual carbon fluxes, especially when they are recovering from past disturbances. Therefore, the most appropriate initialization would be to prescribe observed soil carbon pools for which we do not have enough global data. Thus, although initialization to near steady state is common practice, it is also an assumption in the modeling method.

Accumulation of carbon due to changes in plant biomass has been reported in a previous paper by

Potter (1999) using the NASA–CASA model. Predicted aboveground biomass (AGB; including leaf and wood C) was estimated at 651 Pg C for the globe. Average carbon storage in AGB was predicted to be highest in broadleaf evergreen forests, mostly in the tropical zones, at more than 12 kg C m^{-2}, followed by mixed coniferous–deciduous forests of the temperate zones. Net terrestrial losses of CO_2 from changes in the world's forest ecosystems are between 1.2 and 1.3 Pg C $year^{-1}$ for the early 1990s. This estimate includes areas of forest regrowth and expansion as carbon sinks in temperate and boreal forest zones based on the recent global maps for observed climate, soils, plant cover, and changes in forest areas from natural and human forces.

3. Model results for terrestrial carbon fluxes

For comparison purposes, we define the continental areas for both North America (NA) and Eurasia (EA) as latitude zones higher than 13.5°N within their respective western and eastern sides of the Atlantic Ocean. The southern hemisphere tropical (SHT) zone is defined as the latitudes between the equator and 30°S across the entire globe. In terms of predicted NPP for these areas, the NA continent was estimated to vary between 6 and 7.5 Pg C per year, the EA continent was estimated to vary between 11 and 13 Pg C per year, and the SHT zone was estimated to vary between 16 and 18.5 Pg C per year. Global terrestrial NPP was estimated to vary between 45 and 51 Pg C per year. These results for regional NPP fluxes are all consistent with those reported by Schimel et al. (2001) based largely on predictions from numerous other global ecosystem models and inventories. As further noted by Schimel et al. (2001), the larger NPP fluxes predicted by our model for EA compared to NA are mainly a function of larger total land area coverage over the EA region, rather than higher per unit area NPP fluxes over most of the continents.

Continental and global scale NEP results from NASA–CASA interannual simulations imply the following patterns in ecosystem carbon fluxes:

(a) Since 1982, the terrestrial NEP sink for atmospheric CO_2 in NA has been fairly consistent between +0.2 and +0.3 Pg C per year, except during relatively cool yearly periods like 1987, 1991–1992, and 1995–1996 when the NA continental NEP is predicted to be close to zero net flux of CO_2 (Fig. 3).

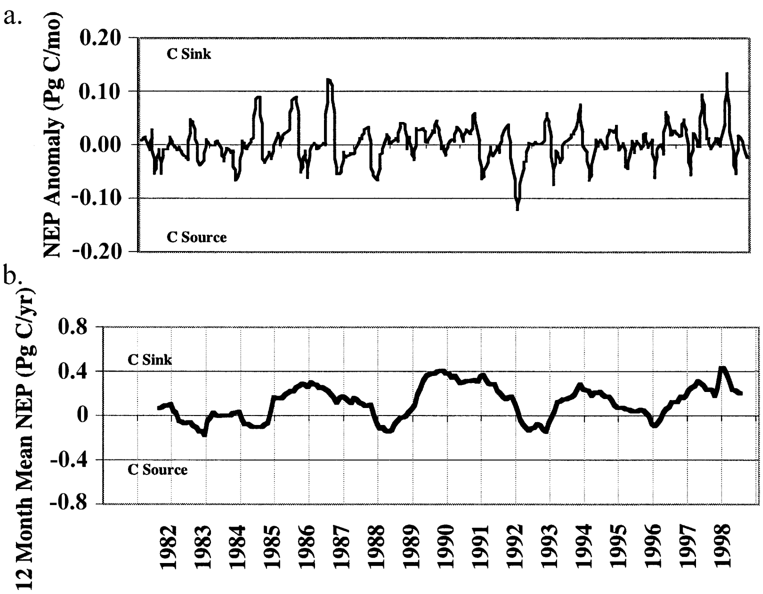

Fig. 3. NASA–CASA results from interannual simulations of NEP for North America. (a) Monthly predictions; (b) 12 month running mean.

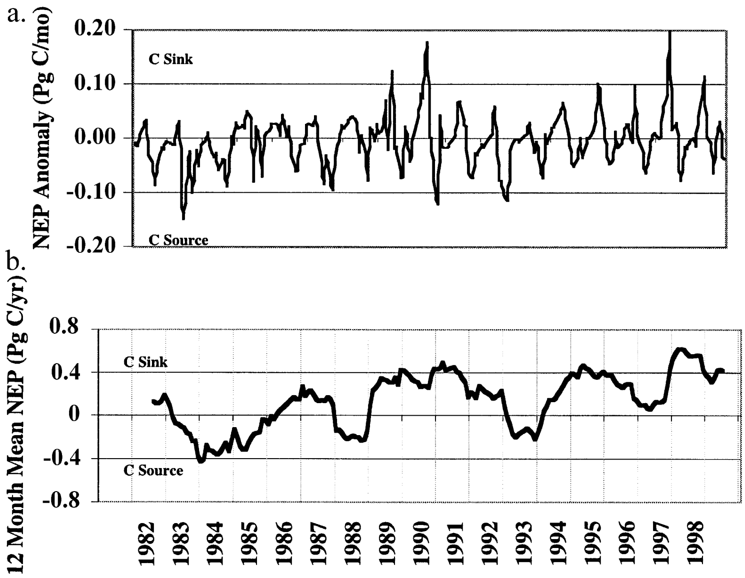

Fig. 4. NASA–CASA results from interannual simulations of NEP for Eurasia. (a) Monthly predictions; (b) 12 month running mean.

(b) The terrestrial NEP sink for atmospheric CO_2 in EA increased notably in the late 1980s and has been fairly consistent between + 0.3 and + 0.55 Pg C per year since 1988, except during relatively cool periods like 1991–1992 and 1995–1996 when the EA continental NEP sink is predicted to vary between + 0.1 and + 0.25 Pg C per year (Fig. 4).

(c) The global NEP flux for atmospheric CO_2 has varied between an annual source of − 0.9 Pg C per year to a sink of + 2.1 Pg C per year (Fig. 5), with the SHT zones having a major influence over global interannual variability (at between − 0.3 and + 0.8 Pg C per year).

(d) The global NEP flux for CO_2 has tended to increase from negative (net source flux to the

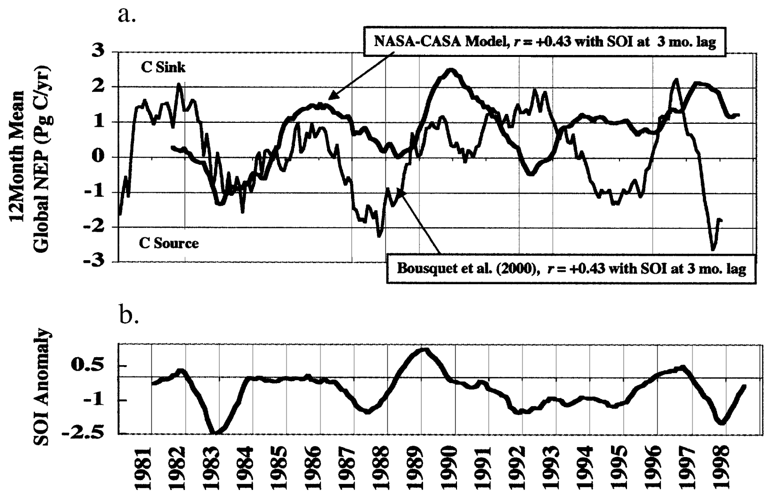

Fig. 5. NASA–CASA global NEP results. (a) 12 month running mean; (b) Southern Oscillation Index, 12 month running mean. Both panels reflect a 12 month offset from actual years of model prediction shown in the *x*-axis.

atmosphere) in the early 1980s to a consistently positive (net sink flux from the atmosphere) by the mid- to late 1990s.

Estimates of net annual carbon sinks for NA reported in this study fall well within the range estimated for continental carbon fluxes assembled by Pacala et al. (2001) and Houghton et al. (1999) mainly from land-based studies. At the global level, comparison of terrestrial NEP flux predictions from NASA–CASA to inverse model estimates for net exchange of atmospheric CO_2 with the terrestrial biosphere (Bousquet et al., 2000) indicates a close agreement from 1982 to 1990 between the two independent methods for estimating net carbon flux on land (Fig. 5). For the period 1991–1995, however, the two modeling predictions diverge markedly, with the NASA–CASA model initially predicting a moderate source flux of CO_2 to the atmosphere followed by a larger sustained sink flux during 1993–1995, and the inverse model predicting essentially the reverse trend. It should be noted that the inverse model estimate can include sources of terrestrial carbon emitted to the atmosphere from ecosystem disturbances, such as wild fires, whereas the NASA–CASA model does not include these additional source fluxes of CO_2. Consequently, because the two models predict somewhat different sub-components of the global carbon cycle, it is possible that both model predictions could be reasonably correct representations of actual fluxes during periods when NASA–CASA predicts a net terrestrial sink for atmospheric CO_2, but the inverse model predicts an additional source flux.

Although our ecosystem modeling results show several consecutive multi-year periods during which the magnitudes of continental sinks for CO_2 were fairly constant, the predicted spatial pattern of these sink fluxes can be highly variable. An example of this result is shown for NA during the years 1996–1998 (Fig. 6). All 3 years are predicted to have continental NEP sink fluxes of 0.1–0.3 Pg C, but the spatial distribution of the annual carbon sink is quite different in each of the 3 years. For example, during 1996, a year not marked by substantial regional warming (compared to 1995) nor by above-average precipitation on a continental scale (Fig. 7), the predicted continental sink for carbon is localized mainly along the eastern portions of the United States and southern Canada. In 1997, substantial regional warming and above-average precipitation were observed, leading to a shift in the major sink areas on the continent to northwestern Canada and portions of the central United States. In 1998, a year closely matching 1997 in total NEP flux of about +0.2 Pg C for NA, regional warming continued and above-average precipitation was observed, leading to another shift in the major sink areas on the continent to southeastern portions of Canada and the United States. These variable spatial patterns of annual carbon sinks within a continental area, which are nearly the same in total flux magnitude, can be investigated in greater detail by examining impacts of large-scale climate dynamics, like El Niño events and global teleconnections, on

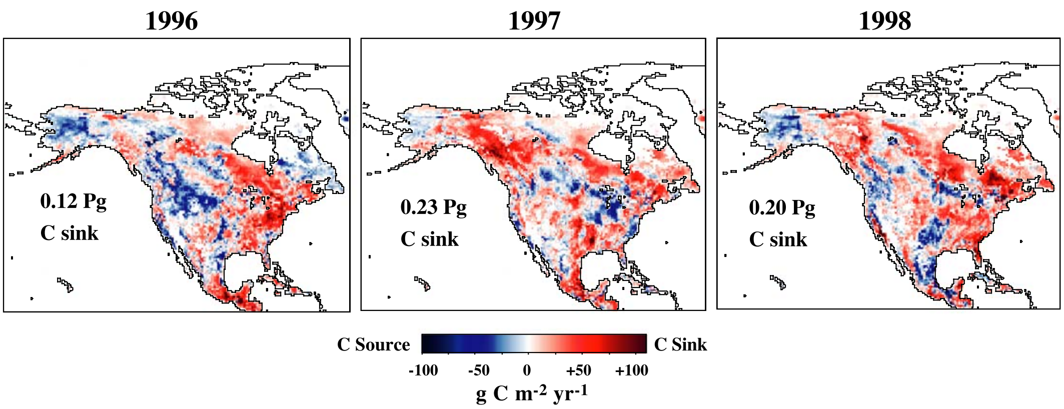

Fig. 6. Predicted interannual variation in annual NEP fluxes for North America, 1996–1998.

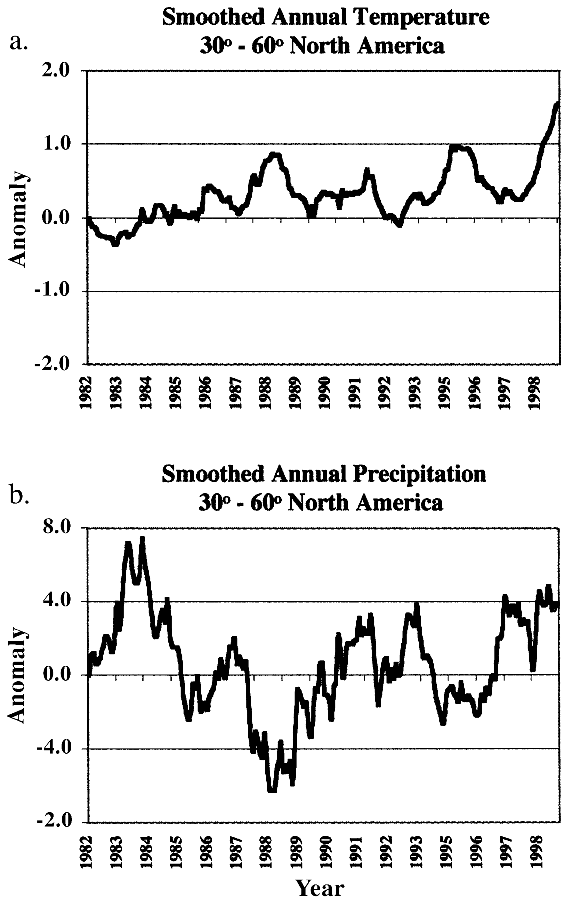

Fig. 7. Smoothed interannual variation in monthly (a) TEMP (12 month running mean), (b) PREC (12 month running sum) for North America, 1982–1998.

the model's climate controller variables (TEMP and PREC) for terrestrial NPP and NEP on regional scales.

4. Understanding global climate controls on ecosystem production

Our NASA–CASA model results are consistent with the findings of McGuire et al. (2001), Vukicevic et al. (2001), and Braswell et al. (1997) that, globally, there appears to be a net release of carbon to the atmosphere during warm and dry El Niño years, and a net uptake during cooler and wetter non-El Niño years. However, our results suggest that this climate control pattern applies mainly to the tropical zones of the terrestrial biosphere. Relatively cool periods in the northern zones (30–60°N) are not commonly associated with net carbon sinks. Vukicevic et al. (2001) postulated that climate warming should increase NPP in northern ecosystems, but that soil R_h should increase more than NPP, leading to decreased or negative NEP. Results from our NASA–CASA model do not strongly support this hypothesis. We find instead that surface warming on the NA and EA continents has increased the observed FPAR and predicted NPP during the 1990s at rates that have exceeded subsequent R_h losses from decomposition. This could result, at least partially, because litterfall (particularly from needleleaf trees), the most labile substrate for decomposition, and responses of soil R_h to climate lag high seasonal NPP fluxes long enough to desynchronize these component fluxes of NEP over time.

4.1. Association analysis for NPP and NEP controllers

Association rule analysis can offer useful insights into the types of dependencies that exist among variables within a large data set. Non-random associations between two or more model variables are reported here using the chi-square test (Stockburger, 1998). Chi-square values greater than 3.84 (degrees of freedom = 1) indicate a high probability ($p < 0.05$) of non-random association between anomalously low (LO) or anomalously high (HI) monthly events for TEMP, PREC, or S_r (solar irradiance) with either NPP or NEP. We used an anomalous event threshold value of 1.5 standard deviations or greater from the long-term (1982–1998) monthly mean value. For our analysis, association patterns are reported below on the basis of frequency of occurrence within major global vegetation types (DeFries et al., 1995).

We find that one of the strongest non-random associations in our NASA–CASA results is that PREC-LO events co-occur with NPP-LO and with NEP-LO events in evergreen broadleaf forests, deciduous broadleaf forests, croplands, and grassland savannas (Fig. 8a). These events occur mainly in drought-sensitive areas of tropical and sub-tropical

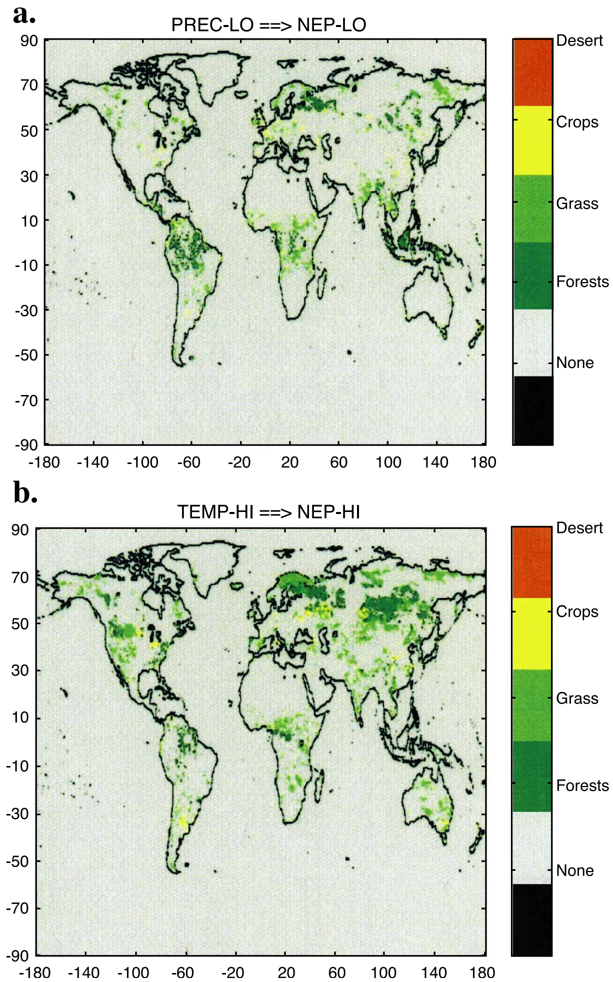

Fig. 8. Locations of co-occurrence between anomalously low (LO) or anomalously high (HI) monthly event observations for climate inputs and NASA–CASA-predicted NEP from 1982 to 1998. An anomalous event threshold value was defined as 1.5 standard deviations or greater from the long-term (1982–1998) monthly mean value. Each non-white pixel indicates a location where NEP anomalies co-occur in the time series with (a) PREC-LO or (b) TEMP-HI, and that the color of that pixel indicates the vegetation type at that location.

zones, and possibly in areas of major wild fires that are associated with FPAR-LO events. We also find that TEMP-HI events co-occur with NPP-LO events for these same vegetation types, which can be another indicator of drought stress effects on plant carbon gains.

Another non-random association rule indicates that TEMP-HI events co-occur with NPP-HI and NEP-HI events in tundra, grasslands, deciduous needleleaf forests, evergreen needleleaf forests, and mixed (needleleaf–broadleaf) forests (Fig. 8b), even with co-occurring PREC-LO events. These observations lead to the hypothesis that regional climate warming has had the greatest impact on high latitude (tundra and boreal) sinks for atmospheric CO_2, particularly over the EA continent.

We find in addition that PREC-HI plus TEMP-HI events co-occur with NPP-HI and NEP-HI events in mixed forests, deciduous broadleaf forests, and evergreen needleleaf forests. This non-random association suggests an important dual control over net carbon fluxes by PREC and TEMP events in transition zones between cool temperate and warmer sub-tropical forest ecosystems.

4.2. Correlations with climate indices

The influence of ocean surface climate events, such as the El Niño Southern Oscillation (ENSO), on atmospheric circulation and land surface climate has been noted as a significant global teleconnection (Glantz et al., 1991). Teleconnection is a term used in meteorological studies to describe simultaneous variation in climate and related processes over widely separated points on earth. There are different phases in climate indices (CIs) such as the ENSO, which is called El Niño in the warm phase and La Niña in the cold phase. ENSO warming at the sea surface, which is driven by changes in winds and ocean–atmosphere heat exchange, typically extends to about 30°N and 30°S latitude, with lags into continental land areas for several months. The Southern Oscillation Index (SOI) is an indicator of atmospheric impacts of ENSO, computed as the standardized difference between sea level pressure (SLP) measured in Tahiti (17°S, 149°W) and Darwin, Australia (13°S, 131°E).

The SOI is commonly used to document warm phases in ENSO, which are often associated with above-average temperatures in the northwestern half of the North American continent, and below-average temperatures in the southeastern half (Trenberth and Hurrell, 1994; Klein et al., 1999; McCabe and Dettinger, 1999). There is also a pattern of the warm-phase ENSO associated with above-average precipitation over western coastal South America (Vuille et al., 2000), the southern United States, and northern Mexico, plus below-average precipitation in south–central Africa, northeastern South America, parts of southern Asia and Australia, and in North America from the Canadian Rockies to the Great Lakes region.

In contrast to ENSO, the North Atlantic Oscillation (NAO) index refers to the north–south oscillation in atmospheric mass between the Icelandic low (65°N, 22°W) and the Azores high pressure centers from 39°N, 9°W to 36°N, 6°W (Walker and Bliss, 1932; Thompson and Wallace, 1998). The atmospheric state indexed by negative NAO corresponds to a southward displacement of winter storms and moisture transport across the North Atlantic into southern Europe (Hurrell, 1995). A positive NAO corresponds to northward displacement of storms and moisture in northernmost Europe and Russia. During winter months when the NAO index is high, anomalously low precipitation commonly occurs over the Canadian Arctic, central and southern Europe, the Mediterranean, and Middle East. Conversely, anomalously high precipitation occurs from Iceland though Scandinavia. In the eastern United States, winters with negative NAO are characterized by more northerly winds, which reduce moisture transports into the region from the south. The NAO can also represent the persistence of below-average temperature variations over North Africa and the Middle East, and above-average temperatures over North America (Hurrell, 1995).

Using matching monthly records for the period of 1982–1998, significant relationships between the time series anomalies of SOI or NAO and carbon (NPP or NEP) fluxes from our NASA–CASA model were identified using Pearson's correlation coefficient (r). In each of these comparison cases, serial correlation (i.e., autocorrelation) needs to be considered when testing the significance of the relationship between two time series. Hence, we first determined the serial correlation of CIs at all possible lag times. SOI anomalies have a low autocorrelation function (< 0.3) at lag times greater than about 6 months (using index data from 1958 to 1995). For NAO anomalies, the autocorrelation function is < 0.1 at lag times greater than 3 months. For our predicted NPP anomalies, the autocorrelation function is < 0.1 at lag times greater than 6 months. Based on these results, we accepted degrees of freedom (df) for the CI time series correlations with NPP and NEP fluxes to be $df = 32$ (34 'seasons' of 6 months duration in a 17-year window, minus 2 for a two-tailed test of significance).

The highest correlations were detected between the deseasonalized time series for SOI with global terrestrial NEP at $r = 0.43$ ($p < 0.05$ with 3 mo lag; Fig. 5), for SOI with SHT NEP at $r = 0.44$ ($p < 0.05$ with 6 mo lag), and for SOI with EA NEP at $r = 0.34$ ($p < 0.05$ with 3 mo lag). In contrast, all global and continental scale correlations between SOI and NPP were found to be low ($r < 0.2$), a pattern also reported by Behrenfeld et al. (2001) using the CASA NPP model, albeit for a much shorter period of 1997–2000. We also found a low correlation between SOI and NA NEP ($r < 0.25$) for 1982–1998. This is not to imply that there were no high correlations between SOI and NPP or NEP time series for many sub-continental areas. On the contrary, on small scales, predicted NPP fluxes from the NASA–CASA model can be highly correlated with

SOI, particularly for areas of the southern United States, northeastern South America, south–central Africa, and parts of southern Asia and Australia.

We could not detect high correlations (r>0.3) between the deseasonalized time series for NAO index with NPP or NEP at either global or continental scales. These results support the hypothesis that the NAO has relatively small-scale effects on interannual variations in land surface climate and terrestrial carbon fluxes, at least compared to ENSO. Areas over northern Canada and the EA continent represent prime examples of these small-scale effects of NAO on predicted NPP from the model.

As implied in the previous section, deseasonalized time series for NPP and NEP fluxes for the entire NA continent were positively correlated with continental TEMP anomalies (Fig. 7), at $r = 0.49$ NPP and at $r = 0.39$ NEP ($p < 0.05$), although not significantly correlated with continental PREC anomalies. Over the same period, continental-scale correlations between SOI or NAO and mean TEMP anomalies were found to be low ($r < 0.15$), whereas the correlation between SOI and continental PREC anomalies was significant ($r = -0.43$; $p < 0.05$). This series of results suggest that teleconnections of commonly used climate indices like SOI and NAO to terrestrial carbon cycles of NA develop as relatively small-scale and temporally varying combinations of climate controls. It also implies that regional climate warming and high latitude (tundra and boreal) sinks for atmospheric CO_2 predicted over NA during the 1990s are not strongly ENSO related.

The relative impacts of PREC, TEMP, and FPAR time series inputs (to the NASA–CASA carbon model) on correlations between climate indices with our predicted NEP fluxes have been examined further in a related paper (Potter et al., in press). For example, we find that 15% of the total land area shown as having a strong correlation of NEP with SOI also shows strong correlation of winter (DJF) PREC with SOI. Just over 34% of total land area shown as having a strong correlation of NEP with SOI also shows strong correlation of TEMP with SOI, while only 7% also shows strong correlation of both PREC and TEMP with SOI. We can therefore conclude that at least 50% of the global land areas shown as having a strong correlation of predicted NEP with climate indices results from similarly strong correlations of either PREC and TEMP model inputs with SOI or NAO. The remaining 50% of the global land area shown as having strong NEP correlations must result from FPAR inputs to the NASA–CASA carbon model, which can also correlate significantly with either climate index.

5. Concluding remarks

Our NASA–CASA model results reveal important patterns of geographic variability in NPP and NEP between and within major continental areas of the terrestrial biosphere. A unique advantage of combining ecosystem modeling with global satellite drivers for vegetation cover properties is to enhance the spatial resolution of sink patterns for CO_2 in the terrestrial biosphere. On the temporal scale, this AVHRR data set used to generate FPAR input to the NASA–CASA model now extends for nearly 20 years of global monthly imagery, which permits model evaluations within the context of other global long-term data sets for climate and atmospheric CO_2 levels. We have begun to identify numerous relatively small-scale patterns throughout the world where terrestrial carbon fluxes may vary between net annual sources and sinks from 1 year to the next. Predictions of NEP for these areas of high interannual variability will require further validation of carbon model estimates, with focus on both flux algorithm mechanisms and potential scaling errors to the regional level.

Acknowledgements

This work was supported by grants from NASA programs in Intelligent Systems and Intelligent Data Understanding, and the NASA Earth Observing System (EOS) Interdisciplinary Science Program. The NASA–CASA model data sets described in this paper are made available for electronic file transfer from geo.arc.nasa.gov.

References

Behrenfeld, M.J., Randerson, J.T., McClain, C.R., Feldma, G.C., Los, S.Q., Tucker, C.I., Falkowski, P.G., Field, C.B., Frouin, R., Esaias, W.E., Kolber, D.D., Pollack, N.H., 2001. Biospheric primary production during an ENSO transition. Science 291, 2594–2597.

Bender, M., Ellis, T., Tans, P., Francey, R., Lowe, D., 1996. Variability in the O2/N2 ratio of southern hemisphere air, 1991–1994: implications for the carbon cycle. Global Biogeochemical Cycles 10, 9–21.

Bonan, G.B., 1989. A computer model of the solar radiation, soil moisture and soil thermal regimes in boreal forests. Ecological Modelling 45, 275–306.

Bousquet, P., Peylin, P., Ciais, P., Le Quéré, C., Friedlingstein, P., Tans, P.P., 2000. Regional changes in carbon dioxide fluxes of land and oceans since 1980. Science 290, 1342–1346.

Braswell, B.H., Schimel, D.S., Linder, E., Moore, B., 1997. The response of global terrestrial ecosystems to interannual temperature variability. Science 278, 870–872.

DeFries, R., Hansen, M., Townshend, J., 1995. Global discrimination of land cover types from metrics derived from AVHRR Pathfinder data. Remote Sensing of Environment 54, 209–222.

Glantz, M.H., Katz, R.W., Nicholls, N. (Eds.), 1991. Teleconnections Linking World-Wide Climate Anomalies. Cambridge Univ. Press, New York, 527 pp.

Goetz, S.J., Prince, S.D., 1998. Variability in light utilization and net primary production in boreal forest stands. Canadian Journal of Forest Research 28, 375–389.

Houghton, R.A., Hackler, J.L., Lawrence, K.T., 1999. The U.S. carbon budget: contributions from land-use change. Science 285, 574–578.

Hurrell, J.W., 1995. Decadal trends in the North Atlantic Oscillation regional temperatures and precipitation. Science 269, 676–679.

IGBP (International Geosphere Biosphere Programme) Terrestrial Carbon Working Group, 1998. The terrestrial carbon cycle: implications for the Kyoto Protocol. Science 280, 1393–1394.

Jumikis, A.R., 1966. Thermal Soil Mechanics. Rutgers Univ. Press, New Brunswick.

Keeling, R.F., Piper, S.C., Heimann, M., 1996. Global and hemispheric CO_2 sinks deduced from changes in atmospheric O_2 concentration. Nature 381, 218–221.

Kindermann, J., Würth, G., Kohlmaier, G.H., 1996. Interannual variation of carbon exchange fluxes in terrestrial ecosystems. Global Biogeochemical Cycles 10, 737–755.

Klein, S.A., Soden, B.J., Lau, N.-C., 1999. Remote sea surface temperature variations during ENSO: evidence for a tropical atmospheric bridge. Journal of Climate 12, 917–932.

Knyazikhin, Y., Martonchik, J.V., Myneni, R.B., Diner, D.J., Running, S.W., 1998. Synergistic algorithm for estimating vegetation canopy leaf area index and fraction of absorbed photosynthetically active radiation from MODIS and MISR data. Journal of Geophysical Research 103, 32257–32276.

Maisongrande, P., Ruimy, A., Dedieu, G., Saugier, B., 1995. Monitoring seasonal and interannual variations of gross primary productivity, net primary productivity, and net ecosystem productivity using a diagnostic model and remotely sensed data. Tellus 47B, 178–190.

Malmström, C.M., Thompson, M.V., Juday, G.P., Los, S.O., Randerson, J.T., Field, C.B., 1997. Interannual variation in global scale net primary production: testing model estimates. Global Biogeochemical Cycles 11, 367–392.

McCabe, G.J., Dettinger, M.D., 1999. Decadal variations in the strength of ENSO teleconnections with precipitation in the western United States. International Journal of Climatology 19, 1399–1410.

McGuire, A.D., Sitch, S., Clein, J.S., Dargaville, R., Esser, G., Foley, J., Heimann, M., Joos, F., Kaplan, J., Kicklighter, D.W., Meier, R.A., Melillo, J.M., Moore III, B., Prentice, I.C., Ramankutty, N., Reichenau, T., Schloss, A., Tian, H., Williams, L.J., Wittenberg, U., 2001. Carbon balance of the terrestrial biosphere in the twentieth century: analyses of CO_2, climate and land-use effects with four process-based ecosystem models. Global Biogeochemical Cycles 15, 183–206.

Monteith, J.L., 1972. Solar radiation and productivity in tropical ecosystems. Journal of Applied Ecology 9, 747–766.

New, M.G., Hulme, M., Jones, P.D., 2000. Representing twentieth-century space–time climate variability: Part II. Development of 1901–1996 monthly grids of terrestrial surface climate. Journal of Climate 13, 2217–2238.

Olson, R.J., Scurlock, J.M.O., Cramer, W., Parton, W.J., Prince, S.D., 1997. From Sparse Field Observations to a Consistent Global Dataset on Net Primary Production. IGBP-DIS Working Paper No. 16, IGBP-DIS. Toulouse, France.

Pacala, S.W., Hurtt, G.C., Baker, D., Peylin, P., Houghton, R.A., Birdsey, R.A., Heath, L., Sundquist, E.T., Stallard, R.F., Ciais, P., Moorcroft, P., Caspersen, J.P., Shevliakova, E., Moore, B., Kohlmaier, G., Holland, E., Gloor, M., Harmon, M.E., Fan, S.-M., Sarmiento, J.L., Goodale, C.L., Schimel, D., Field, C.B., 2001. Consistent land- and atmosphere-based U.S. carbon sink estimates. Science 292, 2316–2320.

Parton, W.J., McKeown, B., Kirchner, V., Ojima, D., 1992. CENTURY Users Manual. Natural Resource Ecology Laboratory. Colorado State University, Fort Collins.

Potter, C.S., 1999. Terrestrial biomass and the effects of deforestation on the global carbon cycle. BioScience 49, 769–778.

Potter, C.S., Klooster, S.A., 1997. Global model estimates of carbon and nitrogen storage in litter and soil pools: response to change in vegetation quality and biomass allocation. Tellus 49B (1), 1–17.

Potter, C.S., Klooster, S.A., 1998. Interannual variability in soil trace gas (CO2, N2O, NO) fluxes and analysis of controllers on regional to global scales. Global Biogeochemical Cycles 12 (4), 621–637.

Potter, C.S., Randerson, J.T., Field, C.B., Matson, P.A., Vitousek, P.M., Mooney, H.A., Klooster, S.A., 1993. Terrestrial ecosystem production: a process model based on global satellite and surface data. Global Biogeochemical Cycles 7, 811–841.

Potter, C.S., Klooster, S.A., Brooks, V., 1999. Interannual variability in terrestrial net primary production: exploration of trends and controls on regional to global scales. Ecosystems 2, 36–48.

Potter, C., Klooster, S., Steinbach, M., Tan, P., Kumar, V., Shekhar, S., Nemani, R., Myneni, R., in review. Global teleconnections of climate to terrestrial carbon flux. J. Geophys. Res.

Priestly, C.H.B., Taylor, R.J., 1972. On the assessment of surface heat flux and evaporation using large-scale parameters. Monthly Weather Review 100, 81–92.

Rayner, P.J., Enting, I.G., Francey, R.J., Langenfelds, R., 1999. Reconstructing the recent carbon cycle from atmospheric CO_2, $d^{13}C$, and O_2/N_2 observations. Tellus 51B, 213–232.

Running, S.W., Nemani, R.R., 1998. Relating seasonal patterns of the AVHRR vegetation index to simulated photosynthesis and transpiration of forests in different climates. Remote Sensing of Environment 24, 347–367.

Schimel, D., House, J., Hibbard, K., Bousquet, P., Ciais, P., Peylin, P., Apps, M., Baker, D., Bondeau, A., Brasswell, R., Canadell, J., Churkina, G., Cramer, W., Denning, S., Field, C., Friedlingstein, P., Goodale, C., Heimann, M., Houghton, R.A., Melillo, J., Moore III, B., Murdiyarso, D., Noble, I., Pacala, S., Prentice, C., Raupach, M., Rayner, P., Scholes, B., Steffen, W., Wirth, C., 2001. Recent patterns and mechanisms of carbon exchange by terrestrial ecosystems. Nature 414, 169–172.

Sellers, P.J., Tucker, C.J., Collatz, G.J., Los, S.O., Justice, C.O., Dazlich, D.A., Randall, D.A., 1994. A global 1×1 NDVI data set for climate studies: Part 2. The generation of global fields of terrestrial biophysical parameters from the NDVI. International Journal of Remote Sensing 15, 3519–3545.

Stockburger, D.W., 1998. Introductory Statistics: Concepts, Models, And Applications, WWW Version 1.0, http://www.psychstat.smsu.edu/sbk00.htm.

Thompson, D.W.J., Wallace, J.M., 1998. The Arctic Oscillation signature in the wintertime geopotential height and temperature fields. Geophysical Research Letters 25, 1297–1300.

Trenberth, J.W., Hurrell, K.E., 1994. Decadal atmosphere–ocean variations in the Pacific. Climate Dynamics 9, 303–319.

USGCRP, 1999. A U.S. Carbon Cycle Science Plan. In: Sarmiento, J.L., Wofsy, S.C. (Eds.), Report of the Carbon and Climate Working Group, U.S. Global Change Research Program. Washington, DC, 69 pp.

Vuille, M., Bradley, R.S., Keimig, F., 2000. Climate variability in the Andes of Ecuador and its relation to tropical Pacific and Atlantic sea surface temperature anomalies. Journal of Climate 13, 2520–2535.

Vukicevic, T., Braswell, B.H., Schimel, D., 2001. Diagnostic study of temperature controls on global terrestrial carbon exchange. Tellus 53B, 150–170.

Walker, G.T., Bliss, E.W., 1932. World weather V. Memoirs of the Royal Meteorological Society 4, 53–84.

Walker, B., Steffen, W., 1997. An overview of the implications of global change for natural and managed terrestrial ecosystems. Conservation Ecology 1, 2.

Watson, R.T., Noble, I.R., Bolin, B., Ravindranath, N.H., Verardo, D.J., Dokken, D.J. (Eds.), 2000. Land Use, Land-Use Change, and Forestry Special Report of the Intergovernmental Panel on Climate Change. Cambridge Univ. Press, UK, 375 pp.